Nanoscale

COMMUNICATION

View Article Online
View Journal

Cite this: DOI: 10.1039/c6nr01253a

Received 12th February 2016,
Accepted 7th March 2016

DOI: 10.1039/c6nr01253a

www.rsc.org/nanoscale

Dimensionality effects on the luminescence properties of hBN†

Léonard Schué,[a,b] Bruno Berini,[b] Andreas C. Betz,[c,d] Bernard Plaçais,[c] François Ducastelle,[a] Julien Barjon[b] and Annick Loiseau*[a]

Cathodoluminescence (CL) experiments at low temperature have been undertaken on various bulk and exfoliated hexagonal boron nitride (hBN) samples. Different bulk crystals grown from different synthesis methods have been studied. All of them present the same so-called S series in the 5.6–6 eV range, proving its intrinsic character. Luminescence spectra of flakes containing 100 down to 6 layers have been recorded. Strong modifications in the same UV range are observed and discussed within the general framework of 2D exciton properties in lamellar crystals.

Introduction

Black and white graphenes are one-atom thick layers of graphite and hexagonal boron nitride (hBN), respectively. Their remarkable properties are inherited from their two-dimensional (2D) crystal structure and symmetry: graphene is a semimetal populated by massless chiral Dirac fermions while hBN is a large band gap semiconductor (>6 eV). As an ultimate 2D crystal, single-layer graphene (SLG) is highly sensitive to its environment and its unique properties can easily be spoiled, but may also be enhanced by the close proximity of a substrate. Therefore, having mostly understood the potential of intrinsic graphene, the new challenge is to engineer its coupling to substrates[1,2] and exploit it to realize innovative electronic and optoelectronic devices. It has become quite clear in recent years that the most compatible environment for graphene is hBN, due to both its insulating character and its similar honeycomb crystal structure, which matches almost perfectly that of graphene.[3–5] Further graphene and hBN have excellent material characteristics, in particular a strong sp^2 bonding that sets a robust energy scale for all excitations (electrons, phonons, excitons).

The rise in widely using hBN layers as a substrate or encapsulating layers of graphene is mainly based on their ability to preserve at the best electronic properties of graphene such as the carrier mobility.[3] However, it was recently shown that, when graphene is epitaxially stacked on hBN layers, a strong interlayer coupling can arise, resulting in marked modifications of its electronic properties.[6,7] An appropriate control of the quality and properties of hBN layers, which may be in turn in an interlayer coupling seems, therefore, an essential milestone towards an appropriate use of hBN layers in complex heterostructure architectures and devices.

However, in contrast to graphene, electronic properties of BN materials remain basically to understand. Luminescence spectroscopies are here very useful tools. Dedicated cathodoluminescence (CL) and photoluminescence (PL) experiments at 10 K have been recently developed and used to study BN powders, single crystals and nanotubes.[8–14]

Luminescence of hBN is found to be dominated by near band edge excitonic recombinations, described as S and D lines.[15] The higher-energy S lines, between 5.6 and 5.9 eV, are generally attributed to intrinsic free excitons, whereas the lower-energy D ones, between 5.4 and 5.65 eV, are assigned to excitons trapped in structural defects.[15,16] Very little is known on hBN 2D layers. In 2D crystals, the excitonic effects are generally amplified by the spatial confinement of electrons and holes, and by the decrease of the electrostatic screening. Lamellar crystals have totally original features when compared to standard 3D-semiconductors, even in the confinement regime reached with epitaxial quantum wells. For instance in MoS_2, the band structure evolves from an indirect bandgap in bulk crystals to a direct band gap for the single atomic layer[17] having a 1 eV exciton binding energy.[18] More recently, a similar indirect-to-direct gap crossover has been reported in WS_2 and WSe_2 from few-layer flakes to the single-layer.[19]

[a]Laboratoire d'Etude des Microstructures, ONERA-CNRS, Université Paris-Saclay, 29 avenue de la Division Leclerc, BP 72, 92322 Châtillon Cedex, France. E-mail: annick.loiseau@onera.fr
[b]Groupe d'Etude de la Matière Condensée, UVSQ-CNRS, Université Paris-Saclay, 45 avenue des Etats-Unis, 78035 Versailles Cedex, France
[c]Laboratoire Pierre Aigrain, Ecole Normale Supérieure-PSL Research University, CNRS, Université Pierre et Marie Curie-Sorbonne Universités, Université Paris Diderot-Sorbonne Paris Cité, 24 rue Lhomond, 75231 Paris Cedex 05, France
[d]Hitachi Cambridge Laboratory, JJ Thomson Avenue, CB3 0HE Cambridge, UK
†Electronic supplementary information (ESI) available. See DOI: 10.1039/C6NR01253A

Analogous effects are then expected for hBN for which exciton binding energies up to 2.1 eV have been theoretically predicted for the single layer.[20–24]

Here, we present a study of the luminescence properties of hBN from its bulk form to atomic exfoliated thin flakes. A thorough investigation by cathodoluminescence (CL) at 10 K of different hBN bulk sources is used to highlight the intrinsic origin of the S series. On the basis of our previous experiments,[13] we manage to isolate almost defect-free exfoliated flakes of different thicknesses from 100 layers (L) down to 6L and to explore their intrinsic luminescence by cathodoluminescence. Measurements reveal a strong thickness-dependent evolution of the near band edge emission that provides insight into the nature of the excitonic recombinations in both the bulk and the 2D layers.

Experimental

The bulk hBN materials investigated in this work are from different origins and were synthesized by various growth processes. Commercially available, the Saint-Gobain powder – dedicated to cosmetic applications (TrèsBN® PUHP1108) – was synthesized at high temperature from boric acid and nitrogen source. BN crystallites from HQ-graphene company were also examined (HQ sample). A sample provided by the Laboratoire Multimatériaux et Interfaces (LMI sample) was synthesized following the Polymer Derived Ceramics (PDCs) route utilizing a polymeric precursor converted at high temperature to a ceramic.[25,26] Finally a single crystal grown at high-pressure high-temperature (HPHT) provided by the NIMS[27] was taken as a reference.

The BN sheets studied in this paper were all exfoliated from Saint-Gobain crystallites. Mechanical peeling was used following the method initially developed for graphene.[28] The powder is applied to an adhesive tape, whose repeated folding and peeling apart separates the layers. They are further transferred onto a Si wafer covered with 90 nm of SiO_2, the optimal thickness for imaging BN flakes with a maximal optical contrast.[29] The SiO_2/Si substrates are also covered with a network of Cr/Au finder marks deposited by UV lithography with the AZ5214E photoresist and Joule evaporation in order to facilitate the localization of the flakes. Prior to the layer transfer, the wafer was chemically cleaned with acetone and isopropanol, followed by several minutes of exposure to a O_2 plasma (60 W, $P \leq 12$ nbar). The last step of this preparation renders the SiO_2 surface hydrophilic and more sensitive to water contamination. That is the reason why we prefer to use the optical contrast (OC) for thickness determination after a Atomic Force Microscopy (AFM) calibration procedure on folded parts (see description in ESI†).

The optical properties of BN samples were analyzed by cathodoluminescence using an optical system (Horiba Jobin Yvon SA) installed on a JEOL7001F field-emission gun scanning electron microscope (SEM). The samples are mounted on a GATAN cryostat SEM-stage cooled down to 10 K with a continuous flow of liquid helium. The samples are excited by electrons accelerated at 2 kV with a beam current of 1 nA. Exfoliated layers were measured using either a fixed electron beam excitation, or for the thinnest flakes, a fast e-beam scanning on the sample in order to limit e-beam-induced modifications. The CL emission is collected by a parabolic mirror and focused with mirror optics on the entrance slit of a 55 cm-focal length monochromator. The all-mirror optics combined with a suited choice of UV detectors and gratings ensure a high spectral sensitivity down to 190 nm. A silicon charge-coupled-display (CCD) camera is used to record the spectra. The spectral response of the optical detection setup was measured from 200 to 400 nm using a deuterium lamp (LOT oriel – deuterium lamp DO544J – 30 W) of calibrated spectral irradiance. The system response for each detector/grating combination was then obtained following the procedure described in ref. 30. All spectra reported in this paper are corrected from the system response.

Results

Intrinsic luminescence of bulk hBN

The CL spectra taken from the commercial samples (Saint-Gobain and HQ Graphene), the LMI sample and the reference crystal from NIMS are reported together in Fig. 1. Actually as these samples were synthesized using very different growth techniques whether it is concerning boron and nitrogen precursors, pressure or process temperature, they obviously cannot afford identical defects or impurities, which could act as trapping sites of the excitons.[13,16] Nevertheless, in spite of their differences, for all the samples, we observe a remarquable similar S series emission with the S1, S2, S3 and S4 lines emerging with a maximum at 5.898 eV (210.2 nm), 5.866 eV (211.4 nm), 5.797 eV (213.9 nm) and 5.771 eV (214.8 nm) respectively. Although these lines have been already reported in previous works,[13,15,31] the present comparative study brings a clear proof for the current interpretation attributing an intrinsic origin to the S lines.[15,16]

According to this interpretation, the S emission lines observed in CL and PL have been assigned[15,16] to the theoretical excitons calculated by Arnaud and Wirtz.[20,21,23,24,32] Actually these calculations show that in the case of a perfect hexagonal symmetry, hBN present two doubly degenerate exciton levels, with a lower dark pair and an upper bright one. A symmetry lowering lifts the degeneracies so that four non degenerate levels are obtained.‡

It is not known precisely what is the reason for this symmetry lowering in our case: zero-point motion[21] or Jahn-Teller like effect[15] have been suggested. In any case phonon effects and exciton–phonon couplings should be involved as indicated by the Stokes shift determined from the comparison of absorption measurements with the PL–CL spectra.[33] It should be noticed that these interpretations assume that the main relevant absorption and luminescence processes are related to direct transitions although *ab initio* calculations predict an

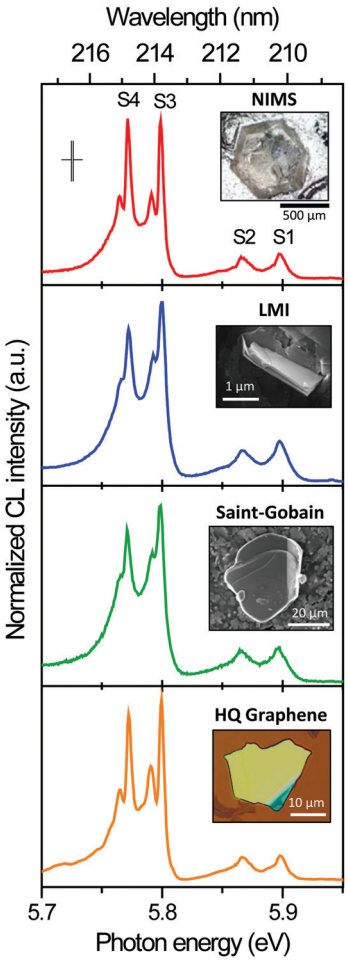

Fig. 1 CL corrected spectra of hBN bulk hBN materials in the near-band-edge region. The reference spectrum of a HPHT high quality single crystal from NIMS is compared to the chemically-grown LMI sample PDCs and the commercial hBN samples. The sample holder temperature is 10 K. All spectra are corrected from the spectral response of the detection system. The spectral resolution is indicated with vertical bars. In insert, typical images of the hBN materials are shown.

indirect gap between points in the Brillouin zone close to the K (and H) point for the valence and close to the M (and L) point for the conduction band. One- or multiphonon processes should perhaps be taken into account.[34]

Finally it is worth mentioning that the excitons described here present similarities with those observed in lamellar transition metal dichalcogenides (TMDs) in which case spin–orbit splitting is clearly observed.[18,35–37] However the spin–orbit splitting should be very weak here for the light B and N elements. Looking at the spectra in more detail, the S3 and S4 emissions exhibit a fine structure splitting with a doublet separated by a few meV and assigned to the transverse and longitudinal components of exciton recombinations, as suggested by polarized-PL experiments.[15] The S3 and S4 doublets are observed leading to the two S4 peaks at 5.762 eV and 5.768 eV and the two S3 peaks at 5.787 eV and 5.794 eV. They can be distinguished in the LMI and the Saint-Gobain powder samples but are better seen in the HQ and the NIMS crystals. This could be due to the fact that the HQ and the NIMS samples were at lower temperature. For practical reasons, they were mounted on a copper plate while the two other ones were mounted on SiO_2/Si substrates of lower thermal conductivity. Indeed, the S peak linewidths have been shown to be strongly dependent on the crystal temperature.[15]

Thickness and luminescence of hBN flakes

Several examples of exfoliated flakes are presented in Fig. 2, 3 and in ESI (Fig. S3†). The uncommon geometry of the exfoliated flake shown in Fig. 2a offers a good configuration to trace the luminescence properties as a function of the hBN thickness in the nanometer range. It displays three atomically-flat regions of 9, 20 and 32 nm thickness as deduced from the AFM profile (Fig. 2b). Assuming a hBN interplanar distance of 0.34 nm and a 1 nm water layer thickness, we estimate that the

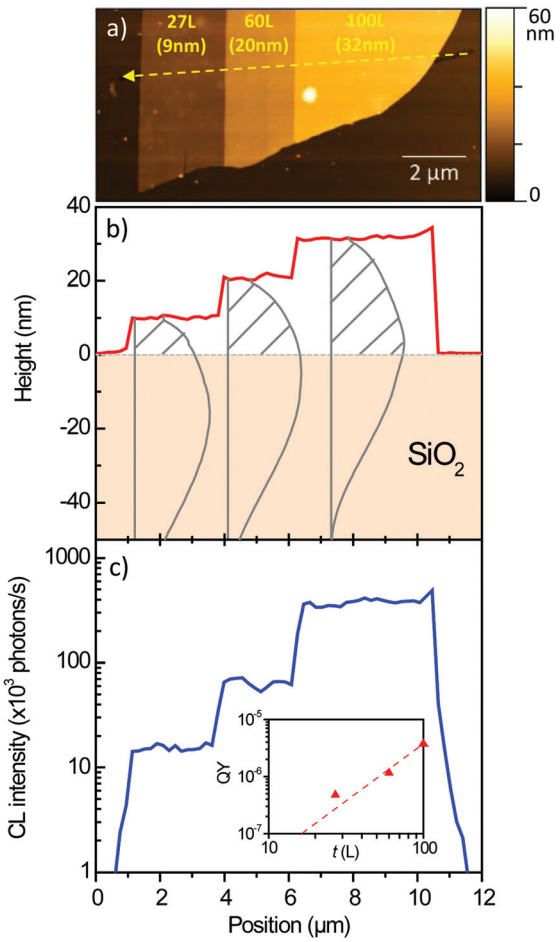

Fig. 2 (a) AFM image of a mechanically exfoliated hBN flake. AFM profile taken along the dotted arrow is depicted in (a). It shows three distinct height steps of 27L (9 nm), 60L (20 nm) and 100L (32 nm) respectively. The depth-dose curves calculated by Monte-Carlo are plotted in gray. (c) CL intensity of S exciton recombinations integrated between 209–217 nm. Inset: plot of the external quantum yield efficiency (QY) for each hBN thickness (details in the text).

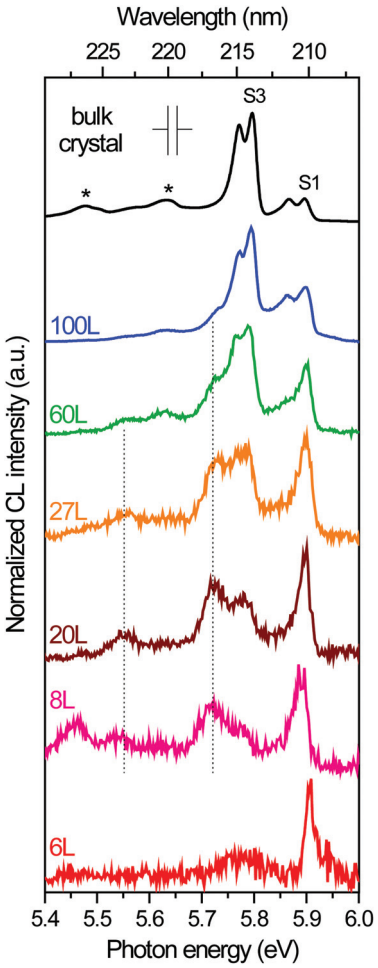

Fig. 3 CL spectra of bulk hBN and flakes of 100, 60, 27, 20, 8 and 6L obtained from the Saint-Gobain material. All spectra are normalized at their maximum intensity and are corrected from the spectral response of the detection system (details in the text). The spectral resolution is indicated with vertical bars. Black dotted lines (resp. stars) indicate the energy position of the first and second phonon replicas of the S1 (resp. S3) line. The sample holder temperature is 10 K.

exfoliated sample is composed of 27, 60 and 100 layers respectively. It is important to notice that the contour outline of the flake is well-defined, suggesting that the hBN crystal is free of any glide defect, which is also confirmed by the absence of the D emission series in the CL spectra.[13,15] This strongly suggests the pristine AA′ stacking of hBN in these three thicknesses. The thickness steps are probably produced by a cleavage perpendicular to the basal plane during the tape removal. Planes with lowest indices (10.0) and (11.0) being the easier to split, the parallel step edges are thus probably oriented along the [11.0] and [10.0] directions respectively in the basal plane corresponding to armchair and zigzag edges respectively. Actually, a recent study reported a statistic of the edges structure in hBN exfoliated flakes and showed a slight preference for zigzag-type edges.[38]

A CL linescan recorded perpendicularly to the step edges is reported in Fig. 2c. The CL intensity clearly decreases when reducing the hBN thickness. Such a result is expected, thin flakes being almost transparent to the electron beam as discussed hereafter.

One of the fundamental differences between CL and PL is that, whereas one absorbed photon generates one electron–hole pair in PL, one single electron generates hundreds of electron–hole pairs in CL. The generation factor G in the hBN thin layer (*i.e.* the number of electron–hole pairs generated per unit time at the bandgap energy) is given by:

$$G = \frac{\alpha V i (1-f)}{\langle E \rangle e} \quad (1)$$

where V is the accelerating voltage, i the electron beam current, e the electronic charge and f the backscattering factor. $\langle E \rangle$ is the average energy required for the formation of an electron–hole pair at the bandgap energy and α is the fraction of energy deposited in the thin hBN layers over the total energy losses (shaded grey area in Fig. 2b over the total integrated area). $\alpha = 1$ in bulk materials, but $\alpha < 1$ for transparent thin layers such as studied here at 2 keV. We will assume $\langle E \rangle \simeq 3E_g$, E_g being the bandgap energy taken equal to 6.4 eV for hBN. Thanks to Monte Carlo simulations using Casino 2.42 software, f and α were calculated using 10^6 electrons. The current i being measured with a Faraday cup, the generation factor G could be estimated: 6.8×10^{10} s^{-1} for a 9 nm layer, 17.9×10^{10} s^{-1} for 20 nm and 31.9×10^{10} s^{-1} for the 32 nm layer. This situation corresponds to the CL linescan over different thicknesses presented in Fig. 2c, where voltage and current are kept constant. The CL intensity, proportional to G, decreases with the layer thickness. This is clearly what we observe in Fig. 2c. It is also remarkable that we obtain an almost homogeneous intensity of S emissions for each step, consistent with the integrity of the hBN crystal after exfoliation.

The external quantum yield (QY) of S intrinsic lines was estimated as a function of the number of hBN layers (shown in inset Fig. 2c). It is calculated as the ratio of the integrated CL intensity of S lines (photons per s) over G (per s) when assuming isotropic light emission and taking into account the aperture of the parabolic mirror (~3.9 steradians). Under such assumptions, we consider this approach provides the order of magnitude of the external quantum yield.

A dependence on the thickness square (t^2) is observed for the QY of exfoliated hBN layers in the inset of Fig. 2c. It is clear that the influence of non-radiative surface recombinations should be considered for discussing the QY values. However it is expected to be proportional to the thickness (t) in the case of thin layers.[39] This indicates that the reported decrease of the quantum yield is not governed by recombinations at the free surface of hBN. While non-radiative recombinations are reported at the surface of sp^3 crystals due the presence of dangling bonds at crystal ends,[39] they are expected to be weak in sp^2 crystals. To explain the t^2 QY dependence, we rather suspect a strong quenching of the luminescence by the SiO_2 substrate, as reported for Frenkel excitons in molecular crystals[40] and perovskites.[41] In practice, this quenching effect

results in the presence of a "dead" hBN layer at the hBN/SiO_2 interface with no contribution to the luminescence. This quenching effect obviously makes difficult luminescence measurements in very thin flakes. As a result, we could record luminescence spectra for flakes thicknesses down to 6L and we have not yet succeeded in getting a significant CL signal in the 1–5 layers thickness range, whatever the sample source. Further we can reasonably consider that in the thinnest flakes investigated, the effective thickness contributing to the luminescence is significantly lower that the geometrical one.

Fig. 3 shows the CL spectra of exfoliated Saint-Gobain crystallites for thicknesses ranging from 100L to 6L. The spectrum of the bulk sample is also plotted for comparison. We stress here that we managed to isolate nanometer-thick hBN layers free of exfoliation defects, which was not the case in our previous work.[13] It is attested by the CL spectra being now all dominated by the S exciton recombinations. Therefore, Fig. 3 well highlights the trend of the thickness dependence extracted from defect-free flakes. Its inspection reveals strong modifications in the CL spectra within the 5.6–6 eV energy range. When reducing the thickness, one can see a progressive and significant decrease of the relative intensities of the S4, S3 and S2 lines compared to the S1 line. At the level of a few monolayers, it is remarkable that the characteristic S4, S3 and S2 lines of bulk hBN almost completely vanished and that in the thinnest 6L flake, S exciton recombinations are reduced to only one emission peak, the S1 line.

It is worth mentioning that this low dimensionality effect is not sample dependent and was in particular confirmed with hBN flakes exfoliated from the NIMS sample (see Fig. S2 of the ESI†) leading to the conclusion that the observed thickness dependence is not governed by defect generation but has rather an intrinsic behavior. The S1 emission, which dominates the luminescence spectra of hBN flakes thinner than 20L, remains particularly sharp. The FWHM of this peak for the 6L sample (17 meV–0.6 nm) corresponds to the spectral resolution with the used experimental conditions.

This evolution of the comparative intensities of S lines is followed by phonon replicas at lower energies. As already reported,[13] phonon replicas of the S3–4 lines are observed in defect-free areas of the bulk hBN material with an energy shift corresponding to the one of the LO phonon mode E_{2g} of hBN. These replicas are indicated by black stars in the reference bulk spectrum of Fig. 3. Looking closer to the spectrum for the 100L flake in Fig. 3, a shoulder can be detected on the low energy side of the S4 peak. Upon decreasing thickness, it emerges – together with the S1 line – as a broader peak of about 50 meV linewidth having a maximum at 5.726 eV (216.5 nm).

Faithful assignment of this peak could be done by recording, using higher integration times, CL spectra of exfoliated hBN flakes with 24L and 30L as shown in Fig. 4. We detect peaks at 5.730 eV, 5.559 eV and 5.392 eV with decreasing intensities. These peaks are shifted by a constant energy value of ~170 meV with respect to S1 emission at 5.903 eV. This energy

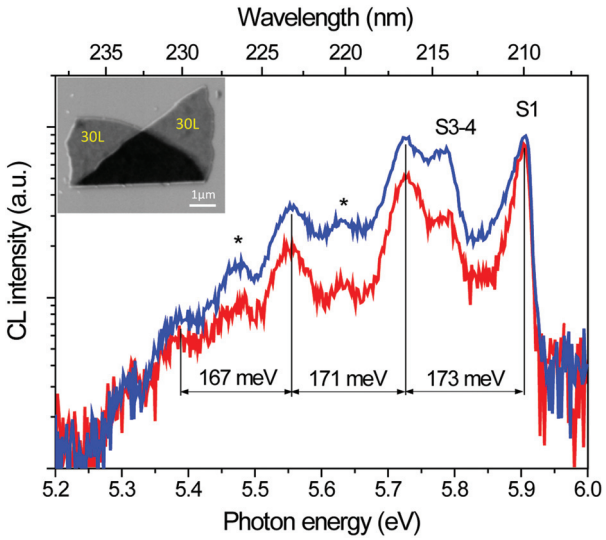

Fig. 4 CL spectra of hBN flakes of 24L (red) and 30L (blue, SEM image in inset) exfoliated from the Saint-Gobain powder. Phonon replicas of the bulk S4 (resp. S1) line are pointed out by black stars (resp. vertical lines). Note that the CL spectra are plotted in logarithmic scale.

almost exactly corresponds to the 169 meV energy of the LO phonon mode E_{2g} of hBN. That this phonon mode is related to in-plane vibrations explains why the number of hBN layers does not affect significantly its energy as shown experimentally[29] and theoretically.[42] Therefore these peaks can be assigned to 3 LO phonon replicas of the S1 line. Looking now again at the thickness evolution in Fig. 3, we identify a complete correlation between the rise of the S1 line and its phonon replicas and the decrease of the S2–4 lines and their phonon replicas. These correlations strongly evidence the reversal of S1 and S2–S4 exciton line intensities when reducing hBN thickness.

This reversal can be further highlighted by plotting the ratio between S1 and S3 luminescence signals for several exfoliated hBN flakes with various thicknesses as shown in Fig. 5. This plot can be considered as the first metrics attempt for quantifying bulk/surface contributions to the luminescence of hBN thin layers. The fit was obtained using the expression $S1/S3 = a/t^{\alpha} + b$ where $b = 0.19$ is a fixed parameter whose value is systematically measured for hBN samples thicker than 1 μm. We found that the best fit is obtained for $\alpha = 0.88$, $a = 19$. Finding a value of α close to 1 is consistent with a surface/volume effect ($1/t$ dependence). This points out the surface origin of the S1 luminescence while the S3 line appears as a characteristic of bulk hBN.

Finally, we observed a small energy shift of the S1 line from 5.871 eV for the bulk to 5.909 eV for the thinnest 6L flake. This shift could be a first indication of a modification in the intrinsic exciton emission energy such as a change in bandgap and/or in exciton binding energy. A similar interpretation has been proposed in a recent study wherein this singular emission at 5.9 eV was observed in large-diameter BNNTs (60 nm).[43]

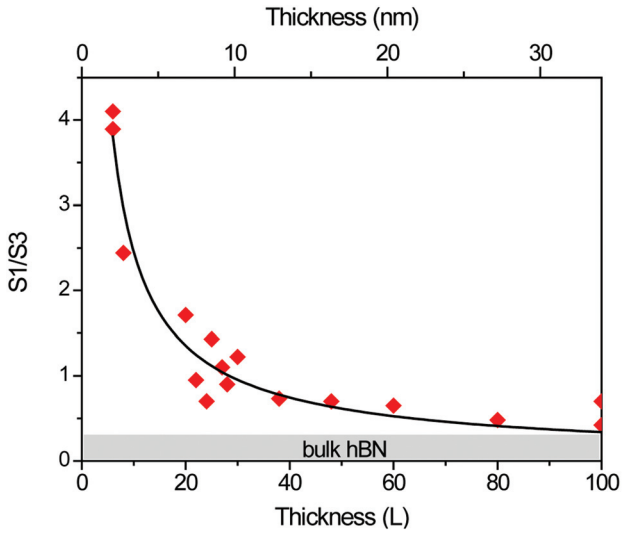

Fig. 5 Ratio between the S1 and S3 luminescence signals as a function of the thickness. The signal amplitudes were measured at 5.898 eV/210.2 nm for the S1 emission and at 5.797 eV/213.9 nm for the S3 emission. The fit curve is described in the text.

Discussion

To summarize analyses presented above, cathodoluminescence performed at 10 K on hBN SiO_2 supported exfoliated flakes reveals a new intrinsic behavior. This behavior is found to be dominated by a thickness dependence in three ways. First, we evidence an anomalous decay of the near band edge luminescence, related to a quenching effect by the SiO_2 substrate. This effect is suspected to provoke the formation of a dead BN layer at the interface with the SiO_2 substrate, which is an obstacle for measuring luminescence from flakes with less than 6 layers. Despite this difficulty, our measurements have revealed that the second and main effect is related to the nature of the luminescence itself. The relative intensities of the four main lines composing the intrinsic excitonic luminescence strongly depend on the number of layers: only the line with the highest energy, which was the weakest in the bulk, remains in the thinnest layers. Importantly, this behavior is independent of the sample source, attesting the intrinsic character of the observed phenomena. Finally, the remaining emission line in the thinnest flakes is observed to be slightly blue shifted.

These three main features obviously shed a new light on the nature of the excitonic emission in hBN, which is far to be completely understood and for which various and controversial analyses have been put forward in the last decade.[8,12,13,15]

A comprehensive interpretation of these results requires theoretical modeling beyond the available calculations in the literature. This will be the subject of a forthcoming article. Here, we just bring to the discussion a few key elements.

First, regarding the luminescence efficiency, the situation of BN on SiO_2 is in contrast to that of suspended MoS_2 layers where the quantum yield increases by a factor of 10^4 between 6L and 1L. For BN on SiO_2, quenching effects evidenced in this work, might hide a strong quantum yield increase as already pointed out in the first paper by Mak *et al.* on MoS_2 monolayer[17] and later further investigated by Buscema *et al.*[44] Alternatively, the question rises whether a strong quantum yield increase could basically occur for the BN monolayer, as bulk hBN is a strongly radiative material compared to other indirect gap materials. In fact, it is clear now that the electronic structure alone is not sufficient to explain hBN luminescence properties and that unusually strong excitonic effects are involved.

We now turn to the thickness dependent behavior of S lines. As recalled previously, all available *ab initio* calculations agree to predict that the four main lines composing the S lines in the bulk are issued from two double degenerate exciton levels, the degeneracy being lifted by exciton–phonon couplings according to a process which is not yet fully elucidated. Actually these calculations also predict for the monolayer a direct gap at points K, just as for di-chalcogenides,[32,45–47] but the situation is simpler here since only two bands, the π valence band and the π^* conduction band have to be considered. As a consequence the lowest excitonic state is a double degenerate state with a large binding energy about 2 eV.[23] In the bulk, two double degenerate states arise instead of one, because there are two planes in the lattice (AA′ stacking) which behave optically differently. So to summarize, a reduction in the number of excitonic lines is expected for the monolayer, compared to the bulk, either a single excitonic line or possibly splitted into two components by electron–phonon interactions.

It is therefore tempting to attribute the single S1 line remaining in the thinnest flakes to the predicted excitonic line for the monolayer. Following this interpretation, the presence of a dead layer at the interface with the SiO_2 substrate would explain why the 6L flakes tend to behave as the last monolayer at their surface. Investigation of self-standing flakes is still under progress in order to ascertain this scenario. From the theoretical side, deeper investigations of the properties of the degenerate excitonic states as a function of the number of layers are currently undertaken.

A final comment concerns the small shift in energy of the S1 line between the bulk and the thinnest flake. The only available *ab initio* calculated absorption spectra including excitonic effects shows that the band gap increases with confinement, but the exciton binding energy also does in the same proportion, so that absorption is expected to be in the same energy range for the bulk and the monolayer (+0.2 eV).[23] Given the uncertainty of such calculations, they appear consistent with our observations of energy shifts of the S lines about a few tens of meV, when reducing the number of hBN layers.

Conclusions

In conclusion, intrinsic luminescence of both bulk and exfoliated layers was identified as a function of the number of

layers. Inspection of bulk crystals from several sources confirm that the intrinsic excitonic luminescence is composed of four main lines, the S lines, whereas for BN hexagonal layers it strongly depends on the number of layers and tends towards the theoretically expected behavior of a single layer due to the direct recombination of a free exciton. This thickness dependent behavior reveals a new face of the excitonic emission in hBN and provides an unprecedented spectroscopic characterization of BN layers from the bulk down to a few layers. This work confirms that h-BN displays unique properties within the family of layered semiconductors and paves the way towards future experimental and theoretical investigations of these properties.

Acknowledgements

Catherine Journet-Gautier and Berangère Toury-Pierre, from LMI, are warmly acknowledged for providing one of their PDCs samples. Authors thank T. Taniguchi and K. Watanabe from NIMS for providing us a reference HPHT crystal, F. Withers from Manchester University for single, bi and tri-layer hBN samples, C. Vilar for technical help on cathodoluminescence-SEM setup, F. Fossard for helpful discussions and C. Voisin for a careful reading of the manuscript. The research leading to these results has received funding from the European Union Seventh Framework Programme under grant agreement no. 604391 Graphene Flagship. We acknowledge funding by the French National Research Agency through Project No. ANR-14-CE08-0018.

References

‡ There are also dark triplet states which are not discussed here.

1 L. Ju, J. Velasco, E. Huang, S. Kahn, C. Nosiglia, H.-Z. Tsai, W. Yang, T. Taniguchi, K. Watanabe, Y. Zhang, G. Zhang, M. Crommie, A. Zettl and F. Wang, *Nat. Nanotechnol.*, 2014, **9**, 348–352.

2 C. R. Woods, L. Britnell, A. Eckmann, R. S. Ma, J. C. Lu, H. M. Guo, X. Lin, G. L. Yu, Y. Cao, R. V. Gorbachev, A. V. Kretinin, J. Park, L. A. Ponomarenko, M. I. Katsnelson, Y. N. Gornostyrev, K. Watanabe, T. Taniguchi, C. Casiraghi, H.-J. Gao, A. K. Geim and K. S. Novoselov, *Nat. Phys.*, 2014, **10**, 451–456.

3 C. R. Dean, A. F. Young, I. Meric, C. Lee, L. Wang, S. Sorgenfrei, K. Watanabe, T. Taniguchi, P. Kim, K. L. Shepard and J. Hone, *Nat. Nanotechnol.*, 2010, **5**, 722–726.

4 L. Wang, I. Meric, P. Y. Huang, Q. Gao, Y. Gao, H. Tran, T. Taniguchi, K. Watanabe, L. M. Campos, D. A. Muller, J. Guo, P. Kim, J. Hone, K. L. Shepard and C. R. Dean, *Science*, 2013, **342**, 614–617.

5 A. Mishchenko, J. S. Tu, Y. Cao, R. V. Gorbachev, J. R. Wallbank, M. T. Greenaway, V. E. Morozov, S. V. Morozov, M. J. Zhu, S. L. Wong, F. Withers, C. R. Woods, Y.-J. Kim, K. Watanabe, T. Taniguchi, E. E. Vdovin, O. Makarovsky, T. M. Fromhold, V. I. Fal'ko, A. K. Geim, L. Eaves and K. S. Novoselov, *Nat. Nanotechnol.*, 2014, 1–6.

6 M. Yankowitz, J. Xue, D. Cormode, J. D. Sanchez-Yamagishi, K. Watanabe, T. Taniguchi, P. Jarillo-Herrero, P. Jacquod and B. J. LeRoy, *Nat. Phys.*, 2012, **8**, 382–386.

7 W. Yang, G. Chen, Z. Shi, C.-C. Liu, L. Zhang, G. Xie, M. Cheng, D. Wang, R. Yang, D. Shi, K. Watanabe, T. Taniguchi, Y. Yao, Y. Zhang and G. Zhang, *Nat. Mater.*, 2013, **12**, 792–797.

8 K. Watanabe, T. Taniguchi and H. Kanda, *Nat. Mater.*, 2004, **3**, 404–409.

9 K. Watanabe, T. Taniguchi, T. Kuroda and H. Kanda, *Diamond Relat. Mater.*, 2006, **15**, 1891–1893.

10 K. Watanabe, T. Taniguchi, T. Kuroda and H. Kanda, *Appl. Phys. Lett.*, 2006, **89**, 141902.

11 M. Silly, P. Jaffrennou, J. Barjon, J.-S. Lauret, F. Ducastelle, A. Loiseau, E. Obraztsova, B. Attal-Tretout and E. Rosencher, *Phys. Rev. B: Condens. Matter*, 2007, **75**, 085205.

12 P. Jaffrennou, J. Barjon, T. Schmid, L. Museur, A. Kanaev, J.-S. Lauret, C. Zhi, C. Tang, Y. Bando, D. Golberg, B. Attal-Tretout, F. Ducastelle and A. Loiseau, *Phys. Rev. B: Condens. Matter*, 2008, **77**, 235422.

13 A. Pierret, J. Loayza, B. Berini, A. Betz, B. Plaçais, F. Ducastelle, J. Barjon and A. Loiseau, *Phys. Rev. B: Condens. Matter*, 2014, **89**, 035414.

14 A. Pierret, H. Nong, F. Fossard, B. Attal-Tretout, Y. Xue, D. Golberg, J. Barjon and A. Loiseau, *J. Appl. Phys.*, 2015, **118**, 234307.

15 K. Watanabe and T. Taniguchi, *Phys. Rev. B: Condens. Matter*, 2009, **79**, 193104.

16 P. Jaffrennou, J. Barjon, J.-S. Lauret, A. Loiseau, F. Ducastelle and B. Attal-Tretout, *J. Appl. Phys.*, 2007, **102**, 116102.

17 K. F. Mak, C. Lee, J. Hone, J. Shan and T. F. Heinz, *Phys. Rev. Lett.*, 2010, **105**, 136805.

18 D. Y. Qiu, F. H. da Jornada and S. G. Louie, *Phys. Rev. Lett.*, 2013, **111**, 216805.

19 W. Zhao, Z. Ghorannevis, L. Chu, M. Toh, C. Kloc, P.-H. Tan and G. Eda, *ACS Nano*, 2012, **7**, 791–797.

20 B. Arnaud, S. Lebègue, P. Rabiller and M. Alouani, *Phys. Rev. Lett.*, 2006, **96**, 026402.

21 B. Arnaud, S. Lebègue, P. Rabiller and M. Alouani, *Phys. Rev. Lett.*, 2008, **100**, 189702.

22 L. Wirtz, A. Marini, M. Grüning and A. Rubio.

23 L. Wirtz, A. Marini and A. Rubio, *Phys. Rev. Lett.*, 2006, **96**, 126104.

24 L. Wirtz, A. Marini, M. Grüning, C. Attaccalite, G. Kresse and A. Rubio, *Phys. Rev. Lett.*, 2008, **100**, 189701.

25 S. Yuan, B. Toury, C. Journet and A. Brioude, *Nanoscale*, 2014, **6**, 7838–7841.

26 S. Yuan, B. Toury, S. Benayoun, R. Chiriac, F. Gombault, C. Journet and A. Brioude, *Eur. J. Inorg. Chem.*, 2014, 5507–5513.

27 T. Taniguchi and K. Watanabe, *J. Cryst. Growth*, 2007, **303**, 525–529.

28 K. S. Novoselov, A. K. Geim, S. V. Morozov, D. Jiang, Y. Zhang, S. V. Dubonos, I. V. Grigorieva and A. A. Firsov, *Science*, 2004, **306**, 666–669.
29 R. V. Gorbachev, I. Riaz, R. R. Nair, R. Jalil, L. Britnell, B. D. Belle, E. W. Hill, K. S. Novoselov, K. Watanabe, T. Taniguchi, A. K. Geim and P. Blake, *Small*, 2011, **7**, 465–468.
30 M. Pagel, V. Barbin, P. Blanc and D. Ohnenstetter, *Cathodoluminescence in Geosciences*, Springer, 2000.
31 X. K. Cao, B. Clubine, J. H. Edgar, J. Y. Lin and H. X. Jiang, *Appl. Phys. Lett.*, 2013, **103**, 191106.
32 L. Wirtz and A. Rubio, *B–C–N Nanotubes and Related Nanostructures*, Springer, New York, 2009, vol. 6, pp. 105–148.
33 K. Watanabe and T. Taniguchi, *Int. J. Appl. Ceram. Technol.*, 2011, **8**, 977–989.
34 G. Cassabois, P. Valvin and B. Gil, *Nat. Photonics*, 2016, DOI: 10.1038/nphoton.2015.277.
35 M. Xu, T. Liang, M. Shi and H. Chen, *Chem. Rev.*, 2013, **113**, 3766–3798.
36 G. Berghäuser and E. Malic, *Phys. Rev. B: Condens. Matter*, 2014, **89**, 125309.
37 L. Zhang and A. Zunger, *Nano Lett.*, 2015, **15**, 949–957.
38 J. S. Kim, K. B. Borisenko, V. Nicolosi and A. I. Kirkland, *ACS Nano*, 2011, **5**, 3977–3986.
39 J. M. Langer and W. Walukiewicz, *Mater. Sci. Forum*, 1995, **196–201**, 1389–1394.
40 P. E. Shaw, A. Ruseckas and I. D. W. Samuel, *Adv. Mater.*, 2008, **20**, 3516–3520.
41 S. D. Stranks, G. E. Eperon, G. Grancini, C. Menelaou, M. J. P. Alcocer, T. Leijtens, L. M. Herz, A. Petrozza and H. J. Snaith, *Science*, 2013, **342**, 341–344.
42 L. Wirtz, A. Rubio, R. de la Concha and A. Loiseau, *Phys. Rev. B: Condens. Matter*, 2003, **68**, 045425.
43 X. Z. Du, C. D. Frye, J. H. Edgar, J. Y. Lin and H. X. Jiang, *J. Appl. Phys.*, 2014, **115**, 053503.
44 M. Buscema, G. A. Steele, H. S. J. van der Zant and A. Castellanos-Gomez, *Nano Res.*, 2014, **7**, 1–11.
45 X. Blase, A. Rubio, S. G. Louie and M. L. Cohen, *Phys. Rev. B: Condens. Matter*, 1995, **51**, 6868–6875.
46 R. M. Ribeiro and N. M. R. Peres, *Phys. Rev. B: Condens. Matter*, 2011, **83**, 235312.
47 N. Berseneva, A. Gulans, A. V. Krasheninnikov and R. M. Nieminen, *Phys. Rev. B: Condens. Matter*, 2013, **87**, 035404.

